

# Modelling & simulation of an electrochemically mediated biofilm reactor for biogas upgrading

Marzieh Domirani Gamunu Samarakoon Carlos Dinamarca\*

Department of Process, Energy and Environment, University of South-Eastern Norway, Norway,  
{230749, gamunu.arachchige, carlos.dinamarca}@usn.no

## Abstract

In this study, we develop a mechanistic model that contributes to the application of microbial electrochemical synthesis (MES) technology for biogas upgrading. The model considered two reactor compartments- a continuous-flow stirred-tank reactor (CSTR) and an MES biofilm reactor which are coupled through a recycle loop. The modelling of biogas production (i.e. anaerobic digestion (AD) process) in the CSTR follows the most used model for biogas process modelling, ADM-1. The MES biofilm model incorporates microbially active CO<sub>2</sub> reduction to CH<sub>4</sub>. To formulate this reduction reaction rate, the Nernst expression was incorporated as a Monod-type kinetic expression. The simulations demonstrate the basic concepts of coupling MES reactor for biogas upgrade and its limitations. According to the simulation result, maximum CH<sub>4</sub> content of 87 % is achievable with recycling ratios of 0.4 and 0.6 when the biofilm volume-specific area is equal to 0.18 m<sup>2</sup>/m<sup>3</sup>, and 0.36 m<sup>2</sup>/m<sup>3</sup> respectively. However, the conversion of CO<sub>2</sub> to CH<sub>4</sub> results in increased pH and consequently CH<sub>4</sub> production decreases by ~ 40 % compared to AD-CSTR without MES. Therefore, it is essential to maintain a proper pH to prevent the inhibition of AD. The rate of the CO<sub>2</sub> conversion to CH<sub>4</sub> can mainly be constrained by available substrate concentration (dissolved CO<sub>2</sub>). The local potential of the cathode and the volume-specific area above 0.36 m<sup>2</sup>/m<sup>3</sup> have minimum effects.

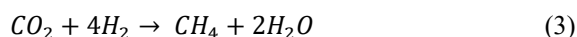
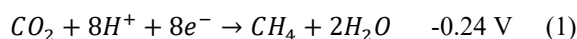
*Keywords: MES, Biofilm, Anaerobic digestion, ADM-1, Bio-methane, Biogas, AQUASIM*

## 1 Introduction

Anaerobic Digestion (AD) is a biological process that produces biogas from organic matter. Biogas contains 50-70 % methane (CH<sub>4</sub>) and 30-50 % carbon dioxide (CO<sub>2</sub>). The CH<sub>4</sub> content has a significant impact on biogas quality; thus, biogas should be purified before using as a transport fuel. Microbial Electrosynthesis (MES) is an effective technology to convert CO<sub>2</sub> to CH<sub>4</sub> with the help of electroactive microorganisms powered by electrical energy (Nelabhotla and Dinamarca, 2018). Thereby the CH<sub>4</sub> content of the biogas can be increased.

The MES cell consists of a cathode as the working electrode and an anode as the counter electrode. The possible chemical reactions of CO<sub>2</sub> conversion to CH<sub>4</sub>

are presented (1-3) with standard potential in Volts (V) vs. Normal Hydrogen Electrode (NHE) (Geppert et al., 2016). The conversion of CO<sub>2</sub> to CH<sub>4</sub> occurs at the cathode through direct electron transfer (1) or indirectly via production of intermediates (2-3). The conversion of CO<sub>2</sub> to CH<sub>4</sub> with intermediate production of hydrogen (H<sub>2</sub>) follows two steps: protons reduction to H<sub>2</sub> and then the produced H<sub>2</sub> is used as an electron donor for CO<sub>2</sub> reduction to CH<sub>4</sub>.



Equation (1) is performed by electroactive microbes growing in the biofilm on the cathode (Siegert et al., 2015). These microorganisms use CO<sub>2</sub> as the only carbon source. Equation (2) can be biotic (Rozendal et al., 2008) or abiotic. The protons (H<sup>+</sup>) and electrons (e<sup>-</sup>) needed for the reduction reaction at the cathode are generated at the anode, by oxidizing water or easily degradable short-chain organics such as acetate. Another possible oxidation compound is ammonium (Sivalingam et al., 2020).

The surface area of the electrodes has a major impact on reactor efficiency. Increasing the cathode surface area can increase the number of catalyst bacteria available and enhance the MES system's efficiency by lowering the biocathode electrode's activation overpotential. Further, a lower potential for the transition of a certain quantity of electrons is more effective than a higher potential for the same amount of electrons (Mueller, 2012). Therefore, direct electron transfer (1) is more desirable than indirect reactions since it occurs at lower potentials.

Even though it is experimentally proved that integrating MES system in AD reactor system can increase the quality of biogas, the technology is still not mature for full-scale implementations. The technology is still to be economically optimized. An MES unit (relatively smaller than a large-scale biogas reactor) can be integrated into an existing AD reactor before a full-scale implementation. Thereby, the technical and economic feasibility of the application can be evaluated. Further, in a unit as such, a pure electroactive methanogenic culture or an enriched methanogenic

consortium can be maintained at the cathode, while the biogas process happens in the main reactor.

This study focuses on a mechanistic modelling approach to study an MES reactor as an auxiliary unit to a main biogas reactor. The experimental work requires significant efforts to test a wide variety of operational conditions, while mathematical modelling can extrapolate such results and enhance our understanding of MES application in the biogas process.

## 2 Materials and methods

Figure 1 shows the reactor configuration of the model. An MES biofilm reactor compartment (MES-RBC) is coupled as an auxiliary unit to a main biogas reactor, which is a continuous-flow stirred-tank reactor (AD-CSTR). The MES-RBC is fed with the effluent from AD-CSTR. The effluent of the MES-RBC is recycled back to AD-CSTR. The reactors are operated under the mesophilic condition (35 °C). The model is formulated in the simulation tool, AQUASIM 2.1.

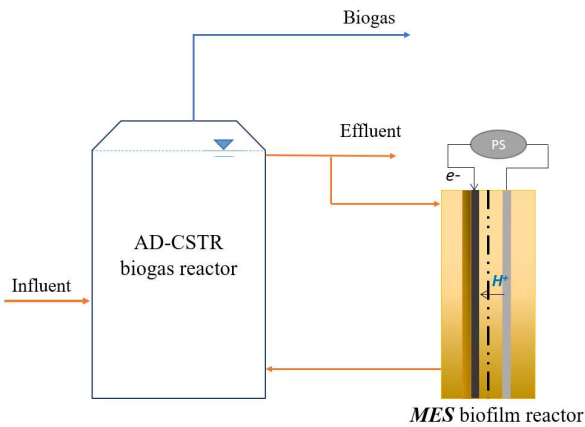


**Figure 1.** Schematic diagram representing MES biofilm reactor coupled with AD-CSTR reactor (for biogas production). CSTR – continuous-flow stirred-tank reactor, AD – Anaerobic digestion, MES - Microbial electrosynthesis, PS – power supply.

### 2.1 AD-CSTR reactor

The main biogas process occurs in AD-CSTR. The reactor has a volume of 28 m<sup>3</sup>. The reactor is fed as described in the simulation outline (Section 2.4). The most common platform for biogas process modelling Anaerobic Digestion Model No.1 (ADM-1) (Batstone et al., 2002) was used to simulate the biogas process in AD-CSTR.

#### 2.1.1 ADM-1 model

The ADM-1 is structured on anaerobic biochemical reactions catalysed by intra or extracellular enzymes and act on the pool of biologically available organic material (Figure 2).

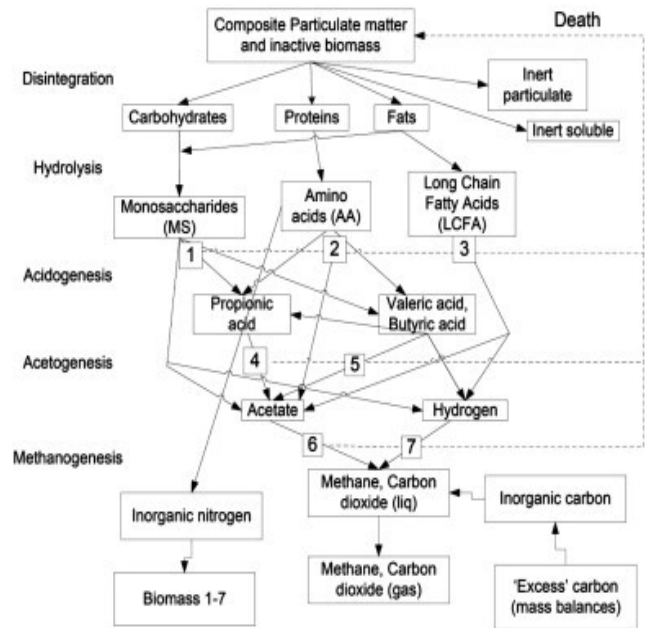


**Figure 2.** The reaction paths in ADM-1 (Batstone et al., 2002), with the following microbial groups: (1) sugar degraders, (2) amino acid degraders, (3) LCFA degraders, (4) propionic acid degraders, (5) butyric and valeric acid (VFA) degraders, (6) acetoclastic methanogens, and (7) hydrogenotrophic methanogens, taken from (Lauwers et al., 2013).

The anaerobic digestion (AD) process decomposes complex organic materials into the final product, biogas (CH<sub>4</sub> and CO<sub>2</sub>) through several decomposition steps. The first step is the disintegration of complex organic material into particulate constituents (carbohydrates, proteins, and lipids). The next step is the hydrolysis of those particulate constituents into soluble sugars, amino acids and long-chain fatty acids (LCFAs). The hydrolysis products are then fermented into volatile fatty acids (acidogenesis step in Figure 2). These acids are broken down to acetate and hydrogen (acetogenesis). The final step is methanogenesis in which acetoclastic methanogens converts acetate to methane, and hydrogenotrophic methanogenesis converts carbon dioxide and hydrogen to CH<sub>4</sub>.

The model incorporates these steps as rate equations. The kinetics of disintegration and hydrolysis steps are expressed as a first-order reaction rate. The substrate uptake rates are described using substrate-level Monod saturation kinetic equations (Monod, 1949). Biomass decay rates for each microorganism type is first order and is described with an independent set of expressions. The detailed description of the model can be found (Batstone et al., 2002).

### 2.2 MES-BRC

The volume of MES-BRC is 2.8 m<sup>3</sup> (10 % of AD-CSTR volume). The reactor is fed with effluent from AD-CSTR, and the flow rate is increased stepwise as a ratio of the effluent flowrate from AD-CSTR.

**Table 1.** Model parameters used for bioelectrochemical processes in MES-BRC according to <sup>a</sup>(Samarakoon et al., 2019); <sup>b</sup>(Processes, 2002); <sup>c</sup>(Reichert, 1998); <sup>d</sup>(Cunningham, 2001); m.d.-determined by the model. MES - Microbial electrosynthesis, RBC - biofilm reactor compartment.

Parameters	Description	Unit	Value
km_eet	maximum electrons uptake rate	Kmol-e Kg COD Xd <sup>-1</sup>	4.5 <sup>a</sup>
X_eet	concentration of electroactive biomass	Kg COD m <sup>-3</sup>	m.d.
S_co2	concentration of dissolved CO <sub>2</sub>	M	m.d.
Ks-co2	Half saturation constant for CO <sub>2</sub> reduction	M	0.06 <sup>a</sup>
F	Faraday's constant	C mol-e <sup>-1</sup>	96485
R	Ideal gas constant	J mol <sup>-1</sup> K <sup>-1</sup>	8.314
T	Temperature	K	308
η	Local potential	V	change
I_NH_limit	Microbial growth inhibition due to limitation of inorganic nitrogen	-	reported formula <sup>b</sup>
Y_eet	Yield of bio-electroactive biomass	Kg COD-X/Kmol-e	0.48 <sup>a</sup>
D_X	Diffusivity of biomass	m <sup>2</sup> d <sup>-1</sup>	1×10 <sup>-7</sup> <sup>c</sup>
D_S_co2	Diffusivity of dissolved CO <sub>2</sub>	m <sup>2</sup> d <sup>-1</sup>	0.00012171
rho	Biomass density	Kg COD m <sup>-3</sup>	25 <sup>c</sup>
LF	Biofilm thickness	m	m.d.
LL	Boundary layer thickness	m	0.0001 <sup>c</sup>
uf	Growth velocity of biofilm	md <sup>-1</sup>	m.d.
A	Cathode biofilm area	m <sup>2</sup>	change
R'	Recycle ratio		change
Kdec_x_eet	first order decay rate of X_eet	d <sup>-1</sup>	0.02 <sup>a</sup>

To simplify the process modelling in MES-BRC, only the chemical reaction which is based on the direct electron transfer process (1), was considered. The electroactive microorganism performs the reaction as microbial growth on a substrate. The specific microbial community in this case is electroactive methanogens which grow on the cathode surface. These bacteria take electrons from the cathode and deliver them to CO<sub>2</sub> as the final acceptor, using CO<sub>2</sub> as a carbon source for biomass growth. As a result, the availability of both the electron donor and the electron acceptor will limit the reaction rate. The overall reaction rate can be defined as (4) detailed in (Samarakoon et al., 2019). The stoichiometric coefficient of this biotic process is the same as in hydrogenotrophic methanogenesis (i.e H<sub>2</sub> uptake) in ADM-1.

$$\rho_{eet} = k_{m-eet}^0 X_{eet} \left( \frac{S_{CO_2}}{K_{S_{CO_2}} + S_{CO_2}} \right) \left( \frac{1}{1 + \exp\left[-\frac{F}{RT}\eta\right]} \right) I_{ph} I_{NH\_limit} \quad (4)$$

$\rho_{eet}$ - kinetic rate. The last term in the parenthesis in (4) which is derived from the Monod equation is referred as the Nernst-Monod term. The main assumption for its use is that microbial kinetics control electron consumption. The Nernst-Monod term shows that the rate of substrate uptake increases as the local potential increases until a constant maximum level is reached.  $R$  is the ideal gas constant,  $T$  is absolute temperature,  $F$  is Faraday constant,  $\eta$  is local potential in reference to  $E_{KA}$ .  $E_{KA}$  is the potential in which the substrate consumption rate will reach half of the

maximum substrate consumption.  $\eta$  is equal to  $\eta = E_{KA} - E_{cathode}$ .  $E_{KA}$  refers to the reference potential ( $E \equiv 0$ ), thus  $\eta = -E_{cathode}$  (Marcus et al., 2007).  $X_{eet}$  is the concentration of electrically active microorganisms,  $I_{ph}$  is an inhibitor that describes microbial growth due to extreme pH conditions,  $I_{NH\_limit}$  is an inhibitor that describes microbial growth due to the limitation of soluble inorganic nitrogen. Other parameters:  $k_{m-eet}^0$  - maximum uptake rate,  $S_{CO_2}$  - dissolved CO<sub>2</sub> concentrations,  $K_{CO_2}$  - half maximum rate concentrations for substrates  $S_{CO_2}$ . In addition to the bio-electrochemical process, decay of electrochemical active biomass  $X_{eet}$  is defined as a process in MES-BRC. The rate ( $dec_{X_{eet}}$ ) is first-order (5) where  $k_{dec-eet}$  is the first-order decay rate.

$$dec_{X_{eet}} = X_{eet} k_{dec-eet} \quad (5)$$

The type of biofilm reactor (in AQUASIM tool) was set to be "confined". The biofilm matrix is a rigid structure with no suspended solid in pore volume. The pore volume consists of only a liquid phase and dissolved solids. The rate of porosity was considered zero. The surface detachment velocity of the biofilm is assumed to be global and set initially as 0.63 times the growth velocity of the biofilm as proposed by (Botheju and Bakke, 2008). More detail about the biofilm reactor compartment in AQUASIM tool can be found in (Wanner and Morgenroth, 2004). Other assumptions made for MES-BRC modelling:

1. The biofilm model is one-dimensional.
2. Biofilm surface area is constant at the given areas (A) for the simulation.
3. The electroactive methanogens catalyze CO<sub>2</sub> reduction to CH<sub>4</sub> (1). This microbial community can acquire electrons directly from the solid cathode.
4. Only the cathodic biofilm in MES-BRC is considered in the modelling (the reaction at the anode is not included).
5. Only electroactive methanogens are present in the biofilm on the cathode surface (any other parallel biochemical and bio-electrochemical reactions are neglected).
6. The inhibition that describes electroactive microbial growth due to extreme pH conditions ( $I_{ph}$ ) is neglected.
7. The anode side (which is not included in the modelling) supplies an unrestricted proton flow and electron current flow (to the cathode side). The transport of H<sup>+</sup> in biofilm is comparatively faster.

### 2.3 Model parameters

The model parameters used for the processes in AD-CSTR are similar to the reported sludge digestion experiment with ADM-1 simulations (Siegrist et al., 2002) and are presented in Table .

### 2.4 Simulation outline

First, a simulation was run only with AD-CSTR without coupling MES-BRC i.e., there was no feed flow to MES-BRC and the processes (4 and 5) were deactivated. The reactor settings of AD-CSTR, and its feed composition were the same as in (Siegrist et al., 2002). The composition of the feed is given in Table 2. The reactor is fed with sludge from a wastewater treatment plant for 50 days (Figure 3). The feed flow increases at day 16 and day 37 (AD reactors are in general started with low organic loading and then gradually increased so that stable reactor operation is achieved).

**Table 2.** Influent feed composition to AD-CSTR.

Compounds	Concentrations kg COD/m <sup>3</sup>
Amino acids	4.2
Fatty acids	6.3
Monosaccharides	2.8
Complex particulates	10.0
Total	23.3

The bio-electrochemical process was activated at day 50 while maintaining a constant feed rate (5.31 m<sup>3</sup>/d) to AD-CSTR. The influent flow to MES-BRC reactor was set as a fraction of effluent from AD-CSTR (i.e., Recycle ratio, R' × effluent flow). The recycle ratio (R') increase stepwise from 0.1 to 0.8 (0.1, 0.2, 0.4, 0.6 and 0.8). The corresponding hydraulic retention times (HRT) for each R' are 5.3, 2.6, 1.3, 0.9 and 0.7 days

respectively. The local cathode potential ( $\eta$ ) was increased from -0.200 to +0.200 V stepwise (step size =0.05) at every 10 days for each recycle ratio. This simulation procedure was followed for 3 different cathodic biofilm areas: 0.5 m<sup>2</sup>, 1 m<sup>2</sup> and 1.5 m<sup>2</sup> which are equal to volume-specific areas of 0.18, 0.36 and 0.54 m<sup>2</sup>/m<sup>3</sup>, respectively.

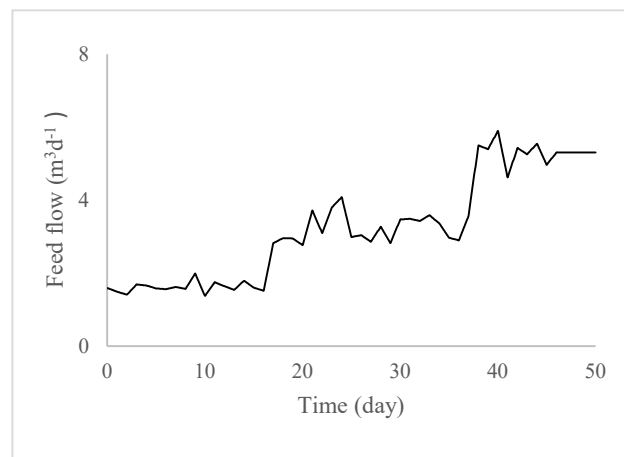


**Figure 3.** The sludge feed flow to AD-CSTR (Siegrist et al., 2002).

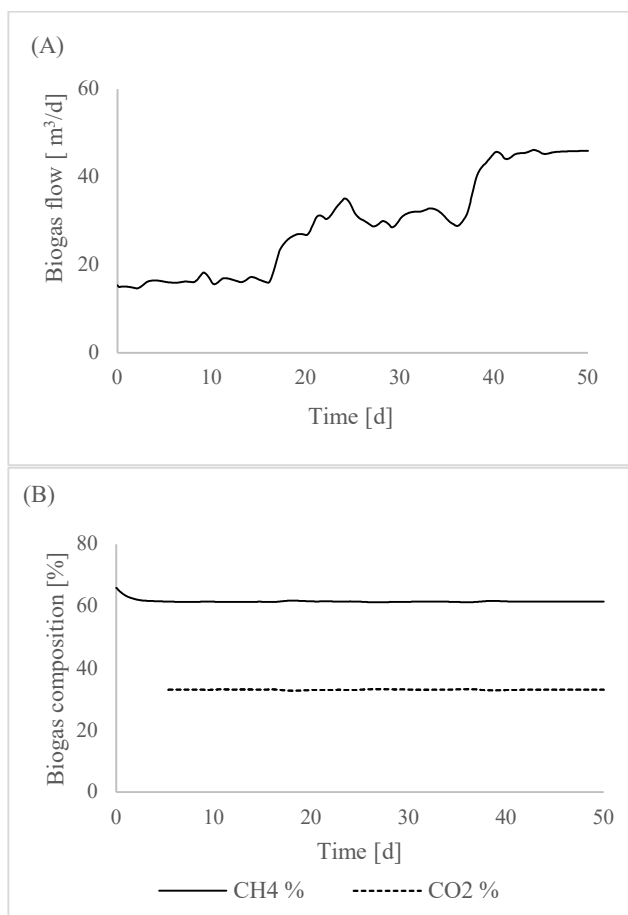
## 3 Results and Discussion

Figure 4 shows the biogas production rate and the composition of the biogas from AD-CSTR when it is not coupled with MES-RBC. As the feed rate is increased during the first 50 days, the biogas production rate increases. The reactor produces biogas ~45m<sup>3</sup>/d at day 50 with ~65 % CH<sub>4</sub> content. This simulation reported (Siegrist et al., 2002) was done for baseline results and the microbial adaptation before any change was made to the conventional biogas process.

Figure 5 shows how the CH<sub>4</sub> content in the biogas from AD-CSTR changes at different recycle ratios (R') when it is coupled with MES-BRC and the local potential of the biocathode varies. CH<sub>4</sub> content increases with the recycle ratio (i.e. the feed flow to MES-BRC increases). The reason is that dissolved CO<sub>2</sub> coming with the recycle flow from the main reactor is converted to CH<sub>4</sub> in MES-BRC and more CH<sub>4</sub> is fed back to AD-CSTR. Increasing local potential ( $\eta$ ) does not make a significant influence on CH<sub>4</sub> content under the condition of this study. This indicates that it is the electron acceptor; in this case, dissolved CO<sub>2</sub> that limits the rate of the conversation reaction (1).

Similarly, the cathodic biofilm area over 1 m<sup>2</sup> does not influence CH<sub>4</sub> content. However, when the area is chosen as 0.5 m<sup>2</sup> and R' is equal to 0.4, the CH<sub>4</sub> content is about 87 % (which is the same at R=0.6). On the other hand, when the area is equal to 1 m<sup>2</sup>, at the same recycle ratio (R= 0.4) the CH<sub>4</sub> content is lower, about 72 %. This indicates that increasing the area from 0.5 to 1 m<sup>2</sup> has given a negative impact on the CO<sub>2</sub> reduction processes. It is in contradiction to the fact that the increased area

provides more biomass available for the conversion processes. A higher cathode area causes higher electron flow and sufficient area for biofilm to grow (Nelabhotla and Dinamarca, 2018; Sydow et al., 2014; Zhang et al., 2019). The reason for this negative influence observed in the current simulation might be due to the larger biofilm thickness at  $A=1 \text{ m}^2$  compared to  $A=0.5 \text{ m}^2$ . Initially higher biomass concentration is available for  $A=1 \text{ m}^2$  compared to  $A=0.5$  and it results in the thicker biofilm for  $A=1 \text{ m}^2$ . Thicker biofilm makes resistance to substrate transfer within the biofilm. This finding suggests the importance of maintaining a proper biofilm thickness in the process. Further, it is also important to properly model the biofilm surface detachment velocity so that an applicable biofilm thickness is maintained.



**Figure 4.** Biogas production rate (A) and its composition (B) from AD-CSTR (when it is not connected with MES-RBC). The feed rate changes at days 16 and 37.

Even though  $\text{CH}_4$  content increases with the recycle ratio, the total biogas production decreases with the recycle ratio (Figure 6, the simulation results are the same for  $A=1$  and  $1.5$ , therefore the result corresponding to  $A=1$  is only presented). In another word, biogas production decreases as  $\text{CH}_4$  content increases. For the case corresponding to the highest  $\text{CH}_4$  content (87%), biogas production decreases by 55% compared to AD-CSTR without MES.

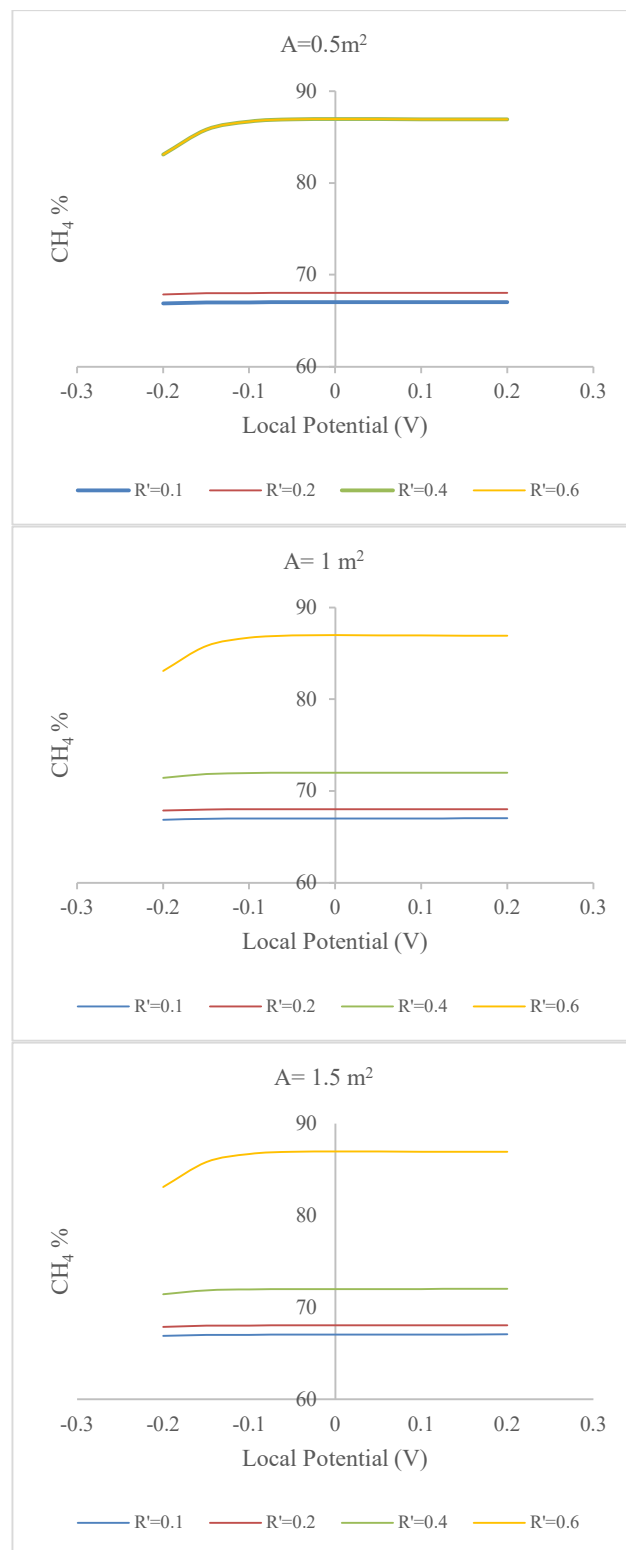


**Figure 5.**  $\text{CH}_4$  content (%) in biogas from AD-CSTR (coupled with MES-RBC) vs. local potential ( $\Pi$ ) from -0.2 to +0.2V (step size=0.05) at different recycle ratios ( $R'$ ) and area ( $A$ )=0.5,1.0 and  $1.5 \text{ m}^2$ .

The increasing recycle ratio allows more  $\text{CO}_2$  from the biogas reactor (AD-CSTR) to convert to  $\text{CH}_4$ . Consequently, bicarbonate strength in the bulk liquid of the reactor (AD-CSTR) decreases and hence pH rises

(Figure 8). The elevated pH can lead to deprotonation of ammonium ions, releasing free ammonia. Free ammonia strictly inhibits acetoclastic methanogens, the bacterial group which is responsible for the decomposition of acetate into methane (Figure 2). In conventional AD, a major portion of biogas is produced via this acetate pathway. When recycle ratio is equal to 0.8, pH rises to 10 (the result is not presented) and acetoclastic methanogens' activity completely terminates. The result is the same for all three biofilm areas studied. However, in the real-case application of MES, the free ammonia can oxidize at the anode (Sivalingam et al., 2020), thereby its inhibition can be mitigated.

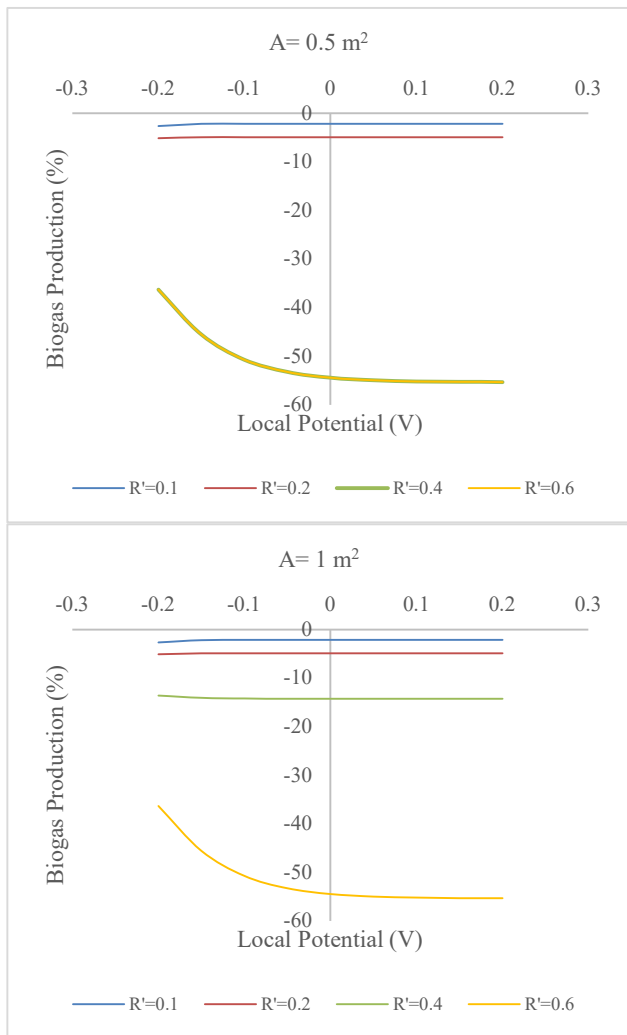


**Figure 6.** Biogas production in AD-CSTR reactor coupled with MES-BRC compared to AD-CSTR without MES when the local potential ( $\Pi$ ) increases from -0.2 to +0.2V (step size=0.05) for different recycle ratios ( $R'$ ) and  $A=0.5$  and  $1\text{m}^2$ .

Due to the reduction in total biogas production in AD-CSTR coupled with MES-BRC, the  $\text{CH}_4$  production also decreases as  $\text{CH}_4$  content increases or the recycle ratio increases (Figure 7, the simulation results are the same for  $A=1$  and  $1.5$ , therefore the result corresponding to  $A=1$  is only presented).  $\text{CH}_4$  production decreases by

40 % at the highest  $\text{CH}_4$  content observed (87 %) at  $R=0.4$  and  $0.6$  when the biofilm area is equal to  $0.5\text{m}^2$  and, at  $R=0.6$  when the biofilm area is equal to  $1\text{m}^2$ . However, a previous experimental study reported that MES could increase  $\text{CH}_4$  yield by 10-15 % compared to that produced in a reactor without MES operation (Nelabhotla and Dinamarca, 2019).

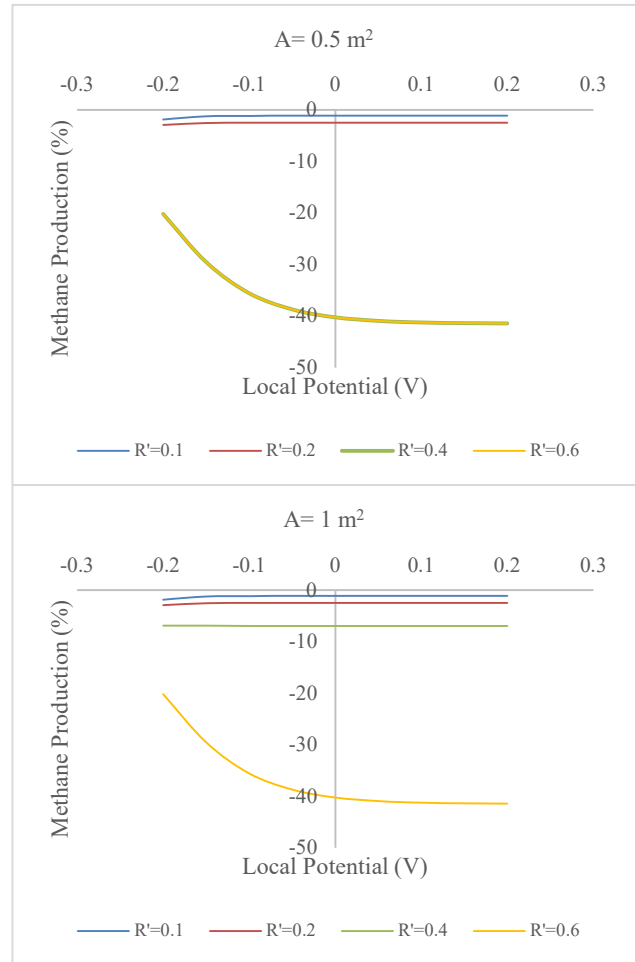


**Figure 7.**  $\text{CH}_4$  production in AD-CSTR reactor coupled with MES-BRC compared to AD-CSTR without MES when the local potential ( $\Pi$ ) increases from -0.2 to +0.2V (step size=0.05) for different recycle ratios ( $R'$ ) and  $A=0.5$  and  $1\text{m}^2$ .

In the present modelling approach, the other processes (both microbial processes and Physico-chemical reactions) in AD were not considered in MES-BRC. If the processes as such were taken into account, the severe impact on biogas production due to pH rise might not be observed, since the AD processes itself can produce some alkalinity/buffer capacity. Further, such a pH rise can also be avoided if extra  $\text{CO}_2$  is added from an external source as suggested by (Samarakoon et al., 2019).

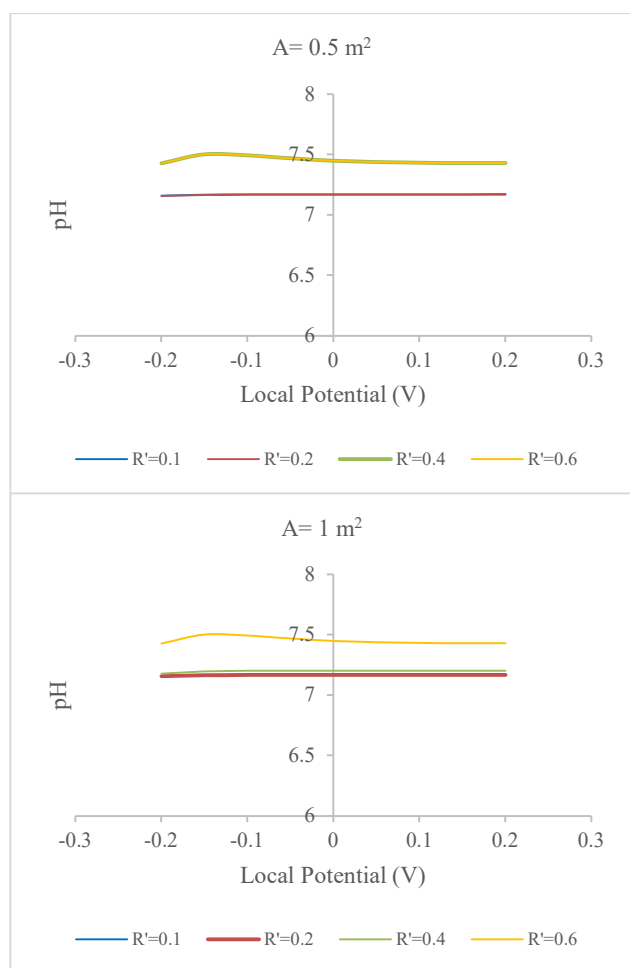


**Figure 8.** Response of pH in AD-CSTR coupled with MES-BRC when the local potential ( $\eta$ ) increases from -0.2 to +0.2V (step size=0.05) for different recycle ratios ( $R'$ ) and  $A=0.5$  and  $1 \text{ m}^2$ .

The diffusion coefficient can also have a significant impact on the  $\text{CO}_2$  reduction rate. To understand the effect of diffusivity on  $\text{CH}_4$  production, low and high values were chosen for the diffusivity coefficient of dissolved  $\text{CO}_2$  for a single simulation case. This examination was done on the case where the local potential is equal to +0.2 V,  $A=1$ , and for all recycle ratios. The high and low diffusivity coefficient values were  $0.002 \text{ m}^2/\text{d}$  and  $0.00002 \text{ m}^2/\text{d}$ , respectively. Only a 0.11% increase in  $\text{CH}_4$  production at the higher value (result not presented) was observed. However, it could be expected that at the lower local potential the diffusivity constant may influence the production.

### 3.1 Limitations of the model and suggestions for improvement.

In the present model, only the bioelectrochemical  $\text{CO}_2$  reduction process and microbial decays are the activated processes in the biofilm reactor (MES-BRC). It means that the model modification assumes only one microorganism ( $X_{\text{cet}}$ ) is growing in the cathodic biofilm, while in the real case, other microorganisms' growth or other microbial processes (Figure 2) also exist.

Both pH and IN have a greater impact on the biological processes. However, the acid-based equilibrium and charge balance (i.e. physicochemical processes) which are vital for pH and inorganic nitrogen (IN) concentration determinations were also not considered in the biofilm modelling (in MES-BRC). Hence, their influence on biofilm growth cannot be studied with the current model. Due to these limitations, the model prediction might be far-off from the real case scenarios even though the model can give a qualitative understanding of the new application.

As a suggestion to improve the model one step further, ADM-1 with the bioelectrochemical  $\text{CO}_2$  reduction process can be implemented in MES-BRC. However, ADM-1 model with AQUASIM software uses a differential-algebraic system of equations (DAE) to model the AD process in CSTR. On the other hand, the solver for the biofilm reactor compartment (BRC) model in AQUASIM cannot numerically handle the DAE system. Therefore, implementing ADM-1 with BRC in AQUASIM is not straightforward. The acid-base equilibrium processes should be removed and redefined as dynamic processes as reported by (Botheju and Bakke, 2008). In Addition, how it will affect ADM-1 with CSTR should also be investigated since the reactor configuration (Figure 1) consists of both CSTR and BRC.

Furthermore, the present model requires proper parameter estimation and validation based on real case scenarios.

## 4 Conclusion

The proposed model can be used to illustrate the principle of MES coupled with AD for biogas upgrading by bio-electrochemically transforming  $\text{CO}_2$  to  $\text{CH}_4$ . The model can be used to study some significant process parameters such as cathode local potential ( $\eta$ ) recycle ratio, cathode area, and biofilm detachment velocity on the MES integrated with AD reactor.

The simulations show that coupling the MES biofilm reactor with a recycle loop increases  $\text{CH}_4$  content in the biogas. The maximum  $\text{CH}_4$  content achieved is 87 % with recycle ratios ( $R'$ ) of 0.4 (1.3 d HRT) and 0.6 (0.9 d HRT) when the biofilm volume-specific area is equal to  $0.18 \text{ m}^2/\text{m}^3$  and  $0.36 \text{ m}^2/\text{m}^3$  respectively (under the reactor condition studied). However, the conversion of  $\text{CO}_2$  to  $\text{CH}_4$  results in elevated pH in the main biogas reactor and consequently  $\text{CH}_4$  production decreases by ~ 40 % compared to AD-CSTR without MES. Therefore, it is essential to maintain a proper pH to prevent the inhibition.

The rate of the  $\text{CO}_2$  conversion to  $\text{CH}_4$  can mainly be constrained by available substrate concentration (dissolved  $\text{CO}_2$ ) and the cathode local potential and volume-specific area above  $0.36 \text{ m}^2/\text{m}^3$  have minimum effects.

## References

- D. J. Batstone, J. Keller, I. Angelidaki, S. V. Kalyuzhnyi, S. G. Pavlostathis, A. Rozzi, W. T. M. Sanders, H. Siegrist, and V. A. Vavilin. The IWA Anaerobic Digestion Model No 1 (ADM1). *Water Science and Technology*, 45(10): 65-73, 2002. doi:10.2166/wst.2002.0292.
- D. Botheju and R. Bakke. Implementation of ADM 1 model in AQUASIM biofilm reactor compartment, 2008. from [www.scansims.org](http://www.scansims.org)
- A. B. A. Cunningham. The Hypertextbook, 2001. Retrieved from [http://www.hypertextbookshop.com/biofilmbook/v005/r001/Contents/01\\_Topics/10\\_Chapter\\_10/02\\_Section\\_2/02\\_Intermediate/01\\_Page\\_1.html](http://www.hypertextbookshop.com/biofilmbook/v005/r001/Contents/01_Topics/10_Chapter_10/02_Section_2/02_Intermediate/01_Page_1.html)
- F. Geppert, D. Liu, M. van Eerten-Jansen, E. Weidner, C. Buisman, and A. ter Heijne. Bioelectrochemical Power-to-Gas: State of the Art and Future Perspectives. *Trends in Biotechnology*, 34(11): 879-894, 2016. doi:<https://doi.org/10.1016/j.tibtech.2016.08.010>.
- J. Lauwers, L. Appels, I. P. Thompson, J. Degève, J. F. Van Impe, and R. Dewil. Mathematical modelling of anaerobic digestion of biomass and waste: Power and limitations. *Progress in Energy and Combustion Science*, 39(4): 383-402, 2013. doi:<https://doi.org/10.1016/j.pecs.2013.03.003>.
- A. K. Marcus, C. I. Torres, and B. E. Rittmann. Conduction-based modeling of the biofilm anode of a microbial fuel cell. *Biotechnology and Bioengineering*, 98(6): 1171-1182, 2007. doi:10.1002/bit.21533.
- J. Monod. The growth of bacterial cultures. *Annual Review of Microbiology*, 3(1): 371-394, 1949. doi:10.1146/annurev.mi.03.100149.002103.
- J. Mueller. (2012). *PhD thesis, Microbial catalysis of methane from carbon dioxide The Future of Renewable Energy is Inside You*. The Ohio State University.
- A. B. T. Nelabhotla and C. Dinamarca. Electrochemically mediated CO<sub>2</sub> reduction for bio-methane production: a review. *Reviews in Environmental Science and Bio/Technology*, 17(3): 531-551, 2018. doi:10.1007/s11157-018-9470-5.
- A. B. T. Nelabhotla and C. Dinamarca. Bioelectrochemical CO<sub>2</sub> Reduction to Methane: MES Integration in Biogas Production Processes. *Applied Sciences*, 9(6): 1056, 2019.
- I. W. A. Task Group for Mathematical Modelling of Anaerobic Digestion Processes. *Anaerobic digestion model no.1 (ADM1)* (Vol. No.13). IWA Publishing, 2002.
- P. Reichert. AQUASIM 2.0-Tutorial. *Swiss Federal Institute for Environmental Science and Technology (EAWAG): Dübendorf, Switzerland*, 1998.
- R. A. Rozendal, A. W. Jeremiasse, H. V. M. Hamelers, and C. J. N. Buisman. Hydrogen Production with a Microbial Biocathode. *Environmental Science & Technology*, 42(2): 629-634, 2008. doi:10.1021/es071720+.
- G. Samarakoon, C. Dinamarca, A. B. T. Nelabhotla, D. Winkler, and R. Bakke. Modelling Bio-Electrochemical CO<sub>2</sub> Reduction to Methane. *SINTEF Proceedings*: 55-61, 2019.
- M. Siegrist, M. D. Yates, A. M. Spormann, and B. E. Logan. Methanobacterium Dominates Biocathodic Archaeal Communities in Methanogenic Microbial Electrolysis Cells. *ACS Sustainable Chemistry & Engineering*, 3(7): 1668-1676, 2015. doi:10.1021/acssuschemeng.5b00367.
- H. Siegrist, D. Vogt, J. L. Garcia-Heras, and W. Gujer. Mathematical Model for Meso- and Thermophilic Anaerobic Sewage Sludge Digestion. *Environmental Science & Technology*, 36(5): 1113-1123, 2002. doi:10.1021/es010139p.
- V. Sivalingam, C. Dinamarca, G. Samarakoon, D. Winkler, and R. Bakke. Ammonium as a Carbon-Free Electron and Proton Source in Microbial Electrosynthesis Processes. *Sustainability*, 12(8): 3081, 2020. doi:10.3390/su12083081.
- A. Sydow, T. Krieg, F. Mayer, J. Schrader, and D. Holtmann. Electroactive bacteria--molecular mechanisms and genetic tools. *Appl Microbiol Biotechnol*, 98(20): 8481-8495, 2014. doi:<https://doi.org/10.1007/s00253-014-6005-z>.
- O. Wanner and E. Morgenroth. Biofilm modeling with AQUASIM. *Water Science and Technology*, 49(11-12): 137-144, 2004. doi:10.2166/wst.2004.0824.
- Z. Zhang, Y. Song, S. Zheng, G. Zhen, X. Lu, T. Kobayashi, K. Xu, and P. Bakonyi. Electro-conversion of carbon dioxide (CO<sub>2</sub>) to low-carbon methane by bioelectromethanogenesis process in microbial electrolysis cells: The current status and future perspective. *Bioresour Technol*, 279: 339-349, 2019. doi:<https://doi.org/10.1016/j.biortech.2019.01.145>.